

# Embeddings and time evolution of the Schwarzschild wormhole

Peter Collas<sup>1</sup> and David Klein<sup>2</sup>

We show how to embed spacelike slices of the Schwarzschild wormhole (or Einstein-Rosen bridge) in  $\mathbb{R}^3$ . Graphical images of embeddings are given, including depictions of the dynamics of this non-traversable wormhole at constant Kruskal times up to, and beyond, the “pinching off” at Kruskal times  $\pm 1$ .

KEY WORDS: Einstein-Rosen bridge, Schwarzschild wormhole, embedding

PACS numbers: 04.20.-q, 04.70.Bw, 02.40.-k, 02.40.Hw

---

<sup>1</sup>Department of Physics and Astronomy, California State University, Northridge, Northridge, CA 91330-8268. Email: peter.collas@csun.edu.

<sup>2</sup>Department of Mathematics, California State University, Northridge, Northridge, CA 91330-8313. Email: david.klein@csun.edu.

# 1 Introduction

The Einstein-Rosen bridge is the prototype example of a wormhole in gravitational physics. It was proposed by Einstein and Rosen [1] in 1935 as a possible geometric model of particles that avoided the singularities of points with infinite mass or charge densities. While not successful as a model for particles, it gained attention after properties of black holes were clarified, and eventually led to the study of traversable wormholes (see, e.g. [2, 3]).

It was not realized until the work of Oppenheimer and Snyder [4] in 1939 that black holes could actually exist, and that they might result from the collapse of sufficiently massive stars. Subsequently in 1962 it was shown by Fuller and Wheeler [5] that the Einstein-Rosen bridge, also called the Schwarzschild wormhole, is part of the geometry of the maximal extension of Schwarzschild spacetime discovered by Kruskal [6] and Szekeres [7], and is non traversable. Reference [5] includes sketches of a sequence of wormhole profiles for various spacelike slices, illustrating the collapse, or “pinching-off”, but the calculations for the embeddings were not included. The main goal of that paper was to demonstrate the impossibility of even a photon passing through the wormhole.

Later in reference [8] essentially the same figures as in [5] were included with some additional variations, and although some hints about the embeddings were given [9], the calculations were again not explained. Two other references, [10] and [11], also provide insights into Schwarzschild wormhole embeddings, but again the mathematical arguments and associated numerical calculations for the dynamics of the wormhole are not presented there, and to our knowledge, are not available in print [12].

In this article, using elementary methods, we show how to embed space slices of the Schwarzschild wormhole in  $\mathbb{R}^3$ . The calculations and examples, apart from supplying the missing material to interested physicists, may be useful in general relativity and differential geometry courses. In Sec. 2, we review Kruskal coordinates for the maximal spacetime extension of Schwarzschild spacetime and display the Schwarzschild metric in this coordinate system. In Sec. 3, we develop a general method for embedding space slices as surfaces of revolution in  $\mathbb{R}^3$ . Section 4 applies that method to embeddings of constant Kruskal times between  $-1$  and  $1$  in order to reveal the full dynamics of the wormhole from formation to collapse. At Kruskal times  $v > 1$ , the two universes, connected by the wormhole at earlier times,  $|v| < 1$ , have separated into two connected components. In Sec. 5 we show how to deal with a technical issue in order to embed space slices of nearly constant Kruskal time  $v > 1$  (or  $v < -1$ ). Then in Sec. 6 we show by example how more general embeddings can be carried out, including an embedding consisting of three separated components. Concluding remarks are given in Sec. 7.

## 2 Kruskal coordinates

Kruskal coordinates  $u, v$  and Schwarzschild coordinates are related by,

$$u^2 - v^2 = \left( \frac{r}{2m} - 1 \right) e^{\frac{r}{2m}}, \quad r \geq 0, \quad (1)$$

and,

$$\frac{2uv}{u^2 + v^2} = \tanh \left( \frac{t}{2m} \right), \quad (2)$$

where  $t$  and  $r$  are the time and radial Schwarzschild coordinates respectively, and the angular coordinates are unchanged. Coordinate  $v$  is timelike and it follows from Eq. (2) that constant ratios  $v/u$  correspond to constant Schwarzschild  $t$ . In Kruskal coordinates, the Schwarzschild metric becomes,

$$ds^2 = \frac{32m^3}{r} e^{-\frac{r}{2m}} (-dv^2 + du^2) + r^2 (d\theta^2 + \sin^2 \theta d\phi^2), \quad (3)$$

where  $r = r(u, v)$  is determined implicitly by Eq. (1), and may be expressed in terms of the *Lambert function* [13] as follows. Dividing both sides of Eq. (1) by  $e$  we may write

$$\zeta = W(\zeta) e^{W(\zeta)}, \quad (4)$$

where in the present case,

$$\zeta = \frac{u^2 - v^2}{e}. \quad (5)$$

The Lambert function,  $W(\zeta)$  is defined to be the function satisfying Eq. (4), i.e., it is the inverse function to  $\zeta(x) = xe^x$ . Then,

$$W \left( \frac{u^2 - v^2}{e} \right) = \frac{r(u, v)}{2m} - 1, \quad (6)$$

and

$$r(u, v) = 2m \left[ 1 + W \left( \frac{u^2 - v^2}{e} \right) \right]. \quad (7)$$

In Fig. 1 we show the maximally extended Schwarzschild spacetime in terms of Kruskal coordinates, with the angular coordinates suppressed, so that each point in the diagram represents a 2-sphere.

The original Schwarzschild coordinates cover only regions I and II in Fig. 1. Region II is the interior of the black hole. Region III is a copy of region I, and region IV is the interior of a white hole. The singularity at  $r = 0$  is given by the ‘‘singularity hyperbola,’’  $v_s(u) = \pm\sqrt{1 + u^2}$ . Additional details may be found, for example, in [8] and [14].

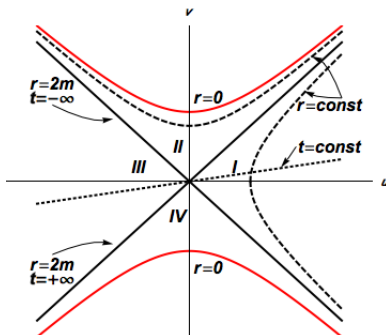


Figure 1: Kruskal diagram of the Schwarzschild geometry.

A particular choice of  $v = v(u)$  as a function of  $u$ , with  $|dv/du| < 1$ , selects a spacelike hypersurface (or a slice) through spacetime, and the projection of the metric of Eq. (3) onto this hypersurface is,

$$ds^2 = \frac{32m^3}{r} e^{-\frac{r}{2m}} \left[ 1 - \left( \frac{dv}{du} \right)^2 \right] du^2 + r^2 (d\theta^2 + \sin^2 \theta d\phi^2). \quad (8)$$

Without loss of generality we shall consider slices with  $v(u) \geq 0$ . For example, choosing  $v(u) = \text{constant}$ , for a range of constants, reveals much of the dynamics of the wormhole, but this simple form for  $v(u)$  is too limiting. As we shall see below, slices with spacetime points with coordinate  $v > 1$ , require special care near the singularity.

### 3 Embedding wormholes as surfaces of revolution in $\mathbb{R}^3$

In order to produce embeddings of two dimensional space slices of the wormhole in  $\mathbb{R}^3$ , we make the restriction  $\theta = \pi/2$ . Specializing to the equatorial plane results in no loss of generality because of the spherical symmetry of Schwarzschild spacetime. With this constraint the metric of Eq. (8) becomes,

$$ds^2 = \frac{32m^3}{r} e^{-\frac{r}{2m}} \left[ 1 - \left( \frac{dv}{du} \right)^2 \right] du^2 + r^2 d\phi^2. \quad (9)$$

Our strategy is to identify Eq. (9) as the metric of a surface of revolution in  $\mathbb{R}^3$  induced by the Euclidean metric. To that end, consider the profile (or generating) curve,  $\alpha(u) = (f(u), 0, g(u))$ , and the associated chart for a surface of revolution,

$$x(u, \phi) = (f(u) \cos \phi, f(u) \sin \phi, g(u)). \quad (10)$$

The induced metric [15] on the surface of revolution is,

$$ds^2 = \left[ (f'(u))^2 + (g'(u))^2 \right] du^2 + f^2(u) d\phi^2. \quad (11)$$

Comparing Eqs. (9) and (11), we make the identifications,

$$f(u) \equiv f(u, v(u)) = r(u, v(u)), \quad (12)$$

and

$$(f'(u))^2 + (g'(u))^2 = \frac{32m^3}{r} e^{-\frac{r}{2m}} \left[ 1 - \left( \frac{dv}{du} \right)^2 \right]. \quad (13)$$

To find  $g(u)$ , we begin by differentiating both sides of Eq. (1) to get,

$$2 \left( u - v \frac{dv}{du} \right) du = \left( \frac{r}{4m^2} \right) e^{\frac{r}{2m}} dr, \quad (14)$$

or

$$du = \frac{\left( \frac{r}{8m^2} \right) e^{\frac{r}{2m}}}{\left( u - v \frac{dv}{du} \right)} dr. \quad (15)$$

Now, assuming that  $v(u)$  is chosen in such a way that  $u$  can be expressed as a function of  $r$  (through Eq.(1)), we may rewrite the metric from Eq. (9) as,

$$ds^2 = \frac{32m^3}{r} e^{-\frac{r}{2m}} \left[ 1 - \left( \frac{dv}{du} \right)^2 \right] \left[ \frac{\left( \frac{r}{8m^2} \right) e^{\frac{r}{2m}}}{\left( u - v \frac{dv}{du} \right)} \right]^2 dr^2 + r^2 d\phi^2. \quad (16)$$

The coefficient,  $g_{rr}$ , of  $dr^2$ , simplifies to

$$g_{rr} = \left( \frac{r}{2m} \right) e^{\frac{r}{2m}} \frac{\left[ 1 - \left( \frac{dv}{du} \right)^2 \right]}{\left[ u - v \frac{dv}{du} \right]^2}. \quad (17)$$

From Eq. (13), and choosing the positive square root, we find that

$$\frac{dg}{du} = \left[ \frac{32m^3}{r} e^{-\frac{r}{2m}} \left[ 1 - \left( \frac{dv}{du} \right)^2 \right] - (f'(u))^2 \right]^{\frac{1}{2}}, \quad (18)$$

and from Eqs. (12), and (15) we have that

$$\frac{df}{du} = \frac{dr}{du} = \frac{8m^2 \left( u - v \frac{dv}{du} \right) e^{-\frac{r}{2m}}}{r}. \quad (19)$$

So Eq. (18) takes the form,

$$\frac{dg}{du} = \left[ \frac{32m^3}{r} e^{-\frac{r}{2m}} \left[ 1 - \left( \frac{dv}{du} \right)^2 \right] - \left[ \frac{8m^2 \left( u - v \frac{dv}{du} \right) e^{-\frac{r}{2m}}}{r} \right]^2 \right]^{\frac{1}{2}}. \quad (20)$$

Eqs. (13), (19), and (20), then give,

$$\left(\frac{g'(u)}{f'(u)}\right)^2 = \left(\frac{dg}{dr}\right)^2 = g_{rr} - 1. \quad (21)$$

Thus, we require  $g_{rr} \geq 1$  (see [11] for a similar observation).

## 4 Constant Kruskal time embeddings before separation of the universes

In this section we consider space slices of the form  $v(u) = v_0$ , for any constant  $v_0 \in [-1, 1]$ . This interval of Kruskal coordinate times captures the full evolution of the wormhole. The spacelike hypersurface at  $v_0 = 0$  may be thought of as a throat, or bridge, joining two distinct, asymptotically flat Schwarzschild manifolds, one depicted in Fig. 1 by regions I and II, and the other by regions III and IV. At this instant, the wormhole has maximum width, with the observer at  $u = 0$  exactly on the event horizon,  $r = 2m$ . As  $v_0$  increases, the observer at  $u = 0$  enters the region  $r < 2m$  and the bridge narrows. When  $v_0 = 1$  the bridge pinches off completely, and the two separating universes just touch at  $r = 0$ . Since the extended spacetime is symmetric in  $v$ , the same evolution occurs in reverse between  $v_0 = -1$  to  $v_0 = 0$ .

For ease of exposition, here and below we will take  $m = 1$ . The embeddings may be carried out using the machinery developed in the previous section. From Eqs. (20) and (21),

$$g(u) = \int_0^u \frac{dg}{du} du = \int_{r(0)}^{r(u)} \frac{dg}{du} \frac{du}{dr} dr, \quad (22)$$

$$= \int_{r(0)}^{r(u)} \sqrt{g_{rr} - 1} dr, \quad (23)$$

$$= \int_{r(0)}^{r(u)} \left[ \frac{2(e^{\frac{r}{2}} - v_0^2)}{re^{\frac{r}{2}} - 2(e^{\frac{r}{2}} - v_0^2)} \right]^{\frac{1}{2}} dr, \quad (24)$$

where  $r(0)$  is given by Eq. (7), i.e.,

$$r(0) = r(0, v_0) = 2 \left[ 1 + W \left( \frac{-v_0^2}{e} \right) \right]. \quad (25)$$

The integral of Eq. (24) can be calculated in closed form for the slice  $v_0 = 0$ . This is the original Einstein-Rosen bridge, and it is typically the only example

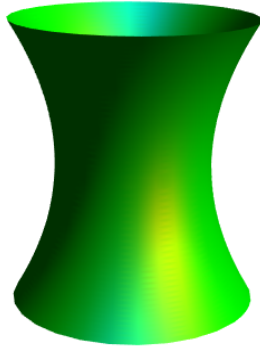


Figure 2: The wormhole embedding for Kruskal time  $v = v_0 = 0.75$ .

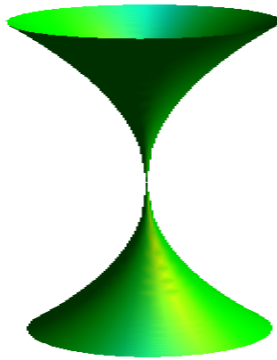


Figure 3: The wormhole at the instant of pinching, i.e.,  $v = v_0 = 1$ .

treated in detail in textbooks [12]. The other embeddings require numerical integrations, and for that purpose we find it convenient to use the first integral in Eq. (22). For the limiting cases  $v_0 = \pm 1$ , the slice meets the singularity tangentially at  $u = 0$ , and that results in an improper integral for  $g(u)$ , which, however, as we show in the next section is convergent. Fig. 2 shows the embedding of the wormhole at Kruskal time  $v_0 = 0.75$ , and Fig. 3 shows it at  $v_0 = 1$ , the instant of pinching off.

## 5 Separated universes at (nearly) constant Kruskal times

In this section we consider the embedding of the wormhole for  $v(u) = v_0$  for constant Kruskal time  $v_0$ , but with  $v_0^2 > 1$ . When  $v_0 < -1$ , the wormhole has not yet formed, and for  $v_0 > 1$ , the wormhole has already formed, then pinched off, and the two universes have separated. We will see that the restriction that  $v(u)$  is constant must be relaxed at space-time points close to the singularity if the embeddings are to include such points.

Since the singularity at  $r = 0$  in Kruskal coordinates is given by the singularity hyperbola  $u^2 - v^2 = -1$ , our function  $v(u) = v_0$  is defined only for the values of  $u$  such that the pair  $(u, v_0)$  (with the angular coordinates suppressed) lies within the Kruskal coordinate chart, i.e, for values of  $u$  that satisfy  $u^2 > v_0^2 - 1$ .

However, the allowable values of  $u$  must be further restricted in order to satisfy the inequality  $g_{rr} \geq 1$  that follows from Eq. (21). To see this, observe that when  $v(u) = v_0$  Eq. (17) reduces to,

$$g_{rr} = \frac{r e^{\frac{r}{2}}}{2u^2}. \quad (26)$$

Combining Eq. (26) with Eqs. (1) and (21) we obtain,

$$\left(\frac{dg}{dr}\right)^2 = \frac{2(e^{\frac{r}{2}} - v_0^2)}{r e^{\frac{r}{2}} - 2(e^{\frac{r}{2}} - v_0^2)}. \quad (27)$$

From this last equation we see that  $r$  must be restricted to those values for which the right-hand side of Eq. (27) is non-negative. It is easily checked that the denominator,  $D(r)$ , of the right-hand side of Eq. (27) satisfies  $D(0) > 0$  and  $D'(r) > 0$  for  $r > 0$ . Therefore,  $D(r) > 0$  for all  $r > 0$ , and the sign of the right-hand side of Eq. (27) is determined solely by the numerator. Therefore we must have  $r > 2 \ln v_0^2$ . Then, using Eq. (1) again, we find that,

$$u^2 \geq v_0^2 \ln v_0^2 \equiv u_0^2. \quad (28)$$

That is, the embedding for  $v(u) = v_0$  is possible for  $u^2 \geq u_0^2 = v_0^2 \ln v_0^2$  only [16].

Our embedding can be extended to include smaller values of  $|u|$ , thus capturing more of the Schwarzschild space-time, if we weaken the restriction that  $v(u)$  is a constant function. To that end, we shall extend  $v(u)$  so that it is a linear function of  $|u|$ , with positive slope, for values of  $u$  with  $u^2 < u_0^2$ . To avoid restrictions of domain analogous to Eq. (28), we consider linear functions that are tangent to the singularity hyperbola,  $v_s(u)$ , as illustrated in Fig. 4. We proceed now to show that this choice enables us to include spacetime points arbitrarily close to the singularity. For simplicity, we restrict our attention to the portion of the spacetime with  $u \geq 0$ . Since we will always take  $v(u)$  to be



an even function, the extension to negative values of  $u$  is straightforward.

Let  $v_1(u) = a_1 u + b_1$  be a linear function that meets the singularity hyperbola,  $v_s(u) = \sqrt{1 + u^2}$ , tangentially at  $u = u_1 \geq 0$ . Then a simple calculation shows that,

$$a_1 = \frac{u_1}{\sqrt{1 + u_1^2}}, \quad b_1 = \frac{1}{\sqrt{1 + u_1^2}}. \quad (29)$$

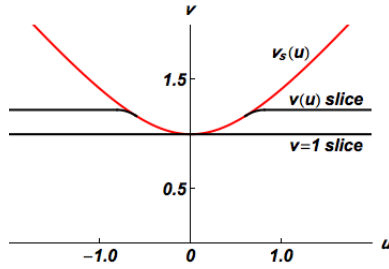


Figure 4: Typical intersections of spacelike slices with the singularity hyperbola  $v_s(u)$ .

With the domain of  $v_1(u)$  temporarily taken to be  $[u_1, \infty)$ , we choose the antiderivative,  $g(u)$  of Eq. (20), as,

$$g(u) = \int_{u_1}^u \frac{dg}{du} du = \int_0^{r(u)} \frac{dg}{dr} dr = \int_0^{r(u)} \sqrt{g_{rr} - 1} dr, \quad (30)$$

where,  $(u_1, v_1)$ , is the point of tangency. From Eq. (17), with  $v = v_1(u)$ , we have that,

$$g_{rr} = \frac{r}{2} e^{\frac{r}{2}} \frac{1 + u_1^2}{(u - u_1)^2}. \quad (31)$$

It is easily verified that,

$$\frac{(u - u_1)^2}{1 + u_1^2} = u^2 - v_1^2(u) + 1 \quad (32)$$

$$= 1 + e^{\frac{r}{2}} \left( \frac{r}{2} - 1 \right), \quad (33)$$

where in the last step we made use of Eq. (1). Substituting Eq. (33) in Eq. (31), we may write the last integral in Eq. (30) as,

$$g(r(u)) = \int_0^{r(u)} \left[ \frac{2(e^{\frac{r}{2}} - 1)}{r e^{\frac{r}{2}} - 2(e^{\frac{r}{2}} - 1)} \right]^{\frac{1}{2}} dr. \quad (34)$$

**Remark.** The integral of Eq. (34) is the same as that in Eq. (24), when  $v(u) \equiv v_0 = 1$ , for which case  $v(u)$  is tangent to the singularity hyperbola at  $r = 0$ .

To see that the integral in Eq. (34) converges and is real, we first note that the same argument applied to Eq. (27) shows that

$$\left(\frac{dg}{dr}\right)^2 \equiv \frac{2(e^{\frac{r}{2}} - 1)}{r e^{\frac{r}{2}} - 2(e^{\frac{r}{2}} - 1)} > 0, \quad (35)$$

when  $r > 0$ . A calculation using L'Hôpital's rule shows that,

$$\lim_{r \rightarrow 0^+} \left[ r \times \left(\frac{dg}{dr}\right)^2 \right] = 4, \quad (36)$$

from which it follows that,

$$\frac{dg}{dr} = \left[ \frac{2(e^{\frac{r}{2}} - 1)}{r e^{\frac{r}{2}} - 2(e^{\frac{r}{2}} - 1)} \right]^{\frac{1}{2}} < \frac{C}{\sqrt{r}}, \quad (37)$$

for  $0 < r < \delta$ , where  $C$  and  $\delta$  are some positive constants. Since the right-hand side of Eq. (37) is integrable, it follows that the integral in Eq. (34) converges.

We may now extend our original constant function  $v(u) = v_0$  by redefining  $v(u)$  to be  $v_1(u)$  for  $u_1 < u \leq u_0$ , and  $v(u) = v_0$  for  $u > u_0$ , for which an embedding function  $g(u)$  may be well defined. However, this extended space slice,  $v(u)$ , fails to be differentiable at  $u_0$ , where it has a kink. To remedy this, we may construct spacelike slices consisting of a straight line segment,  $v = v_1(u)$ , tangent to the singularity hyperbola,  $v_s(u)$ , at  $(u_1, v_1)$  and joined, with the desired degree of smoothness, to another curve,  $v_2(u)$ , (satisfying the spacelike condition,  $|dv_2/du| < 1$ ), which in turn is joined to a constant function,  $v_3(u)$ . The typical situation we have in mind is illustrated in Fig. 5, where the straight line segment,  $v_1(u)$ , is joined to a parabola,  $v_2(u)$ , which in turn is joined at its maximum to a horizontal straight line,  $v_3(u) \equiv v_0$ . In the composite slice the joints are of class  $C^1$ .

For this composite space slice, we have a well defined function  $g(u)$  given by Eq.(30) for  $u \geq 0$ , where as before,  $(u_1, v_1)$  is the point where  $v(u)$  meets the singularity hyperbola. For  $u \leq 0$ ,  $g(u)$  is defined by

$$g(u) = \int_{-u_1}^u \frac{dg}{du} du, \quad u \leq -u_1 \leq 0. \quad (38)$$

Note that since  $v(u)$  is an even function of  $u$ , it follows that  $r(u, v(u))$  and  $dg(u)/du$  are also even functions, and consequently  $g(-u) = -g(u)$ , i.e.,  $g(u)$  is

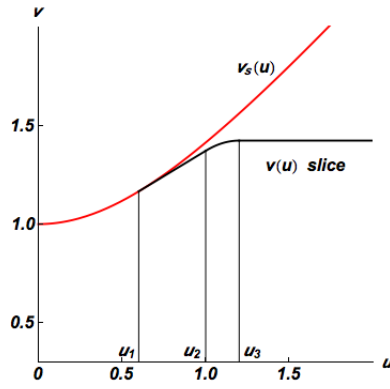


Figure 5: A smooth, nearly constant space slice  $v(u)$  (for  $u > 0$ ) tangential to the singularity.

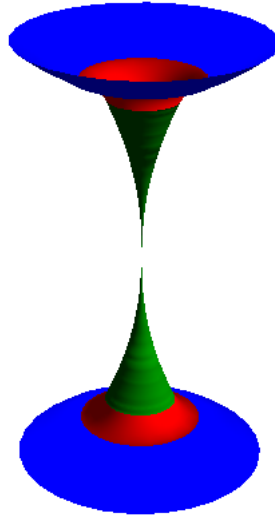


Figure 6: The collapsed wormhole corresponding to Fig. 5. The distance between the pinches is arbitrary.

odd. This observation simplifies the numerical calculations.

Fig. 6 shows an embedding for a space slice,  $v(u)$ , consisting of the three parts illustrated in Fig. 5. The straight line,  $v_1(u)$  of Eq. (29), is tangent to the singularity hyperbola at  $u_1 = 0.6$ . The parabola,  $v_2(u) = v_1(u)$ , at  $u = u_2 = 1.0$

and their slopes match there. The parabola,  $v_2(u)$ , is joined at its maximum,  $u_3 = 1.2$ , to the horizontal straight line,  $v_3(u)$ , whose constant value is approximately 1.424 (and thus the slopes match there also). We have ensured that the joints are of class  $C^1$ , i.e., continuously differentiable.

Another space slice serves both as an alternative to the previous example and as a transition to the next section. Let,

$$v_H(u) = k + \frac{b}{a} \sqrt{(u-h)^2 - a^2}, \quad (39)$$

where we choose  $a = 4$ ,  $b = 1$ . The values  $h \approx -3.5648$ , and  $k \approx 0.84394$  are then determined by our additional requirement that  $v_H(u)$  is tangent to the singularity hyperbola at  $u_1 = 0.8$ , as shown in Fig. 7. This space slice is infinitely differentiable, and analogous to the derivations of Eqs (36) and (37) for the straight line tangent, it can be shown for the present example that,

$$\frac{dg}{du} < \frac{C}{\sqrt{u-u_1}}, \quad (40)$$

for  $0 < u-u_1 < \delta$ , where  $C$  and  $\delta$  are some positive constants [17]. Therefore the integral in Eq. (30) converges. The corresponding embedding of the collapsed wormhole is shown in Fig. 8.

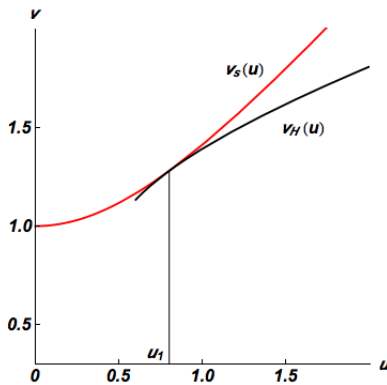


Figure 7: The hyperbola  $v_H(u)$  slice for  $u > 0$ .

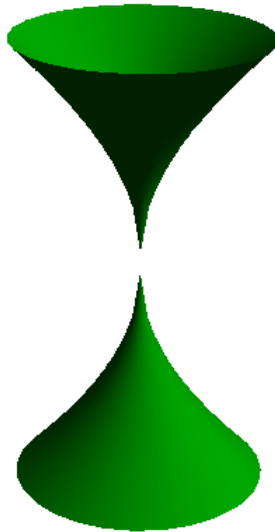


Figure 8: The wormhole of the slice  $v_H(u)$ . The distance between the pinches is arbitrary.

## 6 Three component embeddings

In the previous sections our focus was on embeddings of the Schwarzschild wormhole for constant, or nearly constant, Kruskal times. However, as illustrated in the last example of the previous section, smooth embeddings are also readily available for an unlimited choice of other non constant space slices. As a further illustration, consider a family of space slices defined for all values of  $u$ , whose graphs are again hyperbolae. Let,

$$v(u, v_0) = v_0 + \frac{p}{q} \sqrt{(u^2 + q^2)}. \quad (41)$$

where  $p$  and  $q$  are positive constants, and  $v_0$  is a parameter whose variation may be regarded as representing the time evolution of this family of space slices. For concreteness, we take  $p = q/2$  and  $q = 0.1$ .

We may again use Eq. (20) to calculate  $g(u)$ . The integrations present no special difficulties, but must be done numerically. For the case that  $v_0 \equiv v_{01} = 0.6$ , the slice and corresponding wormhole are shown in Figs. 9 and 10.

Now let  $v_0$  increase until  $v(u, v_0)$  has two points of tangency with the singularity hyperbola, as shown in Fig. 9. This occurs when  $v_0 \equiv v_{02} = 3\sqrt{33}/20$ . As  $v_0$  increases to this value, the cylinder gradually pinches off at two values of  $v$ . The

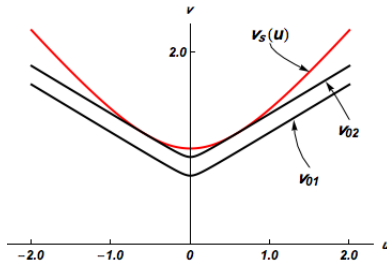


Figure 9: The hyperbolae  $v(u, v_0)$  slices.

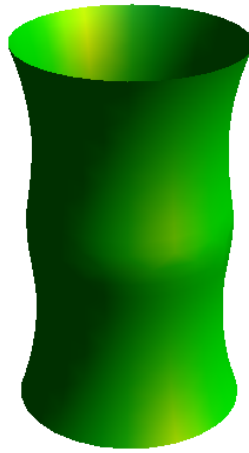


Figure 10: The wormhole of the slice  $v(u, v_0)$ , with  $v_0 = v_{01}$ .

corresponding embedding displayed in Fig. 11 shows a separation of universes into three components. A qualitatively similar model of a collapsing dust star is discussed in detail in Box 32.1 of Ref. [8] (see figure on p. 856).

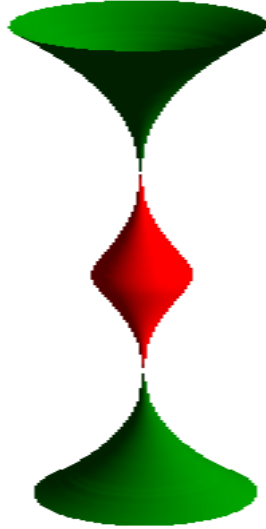


Figure 11: The wormhole of the slice  $v(u, v_0)$ , with  $v_0 = v_{02}$ .

## 7 Concluding remarks

Using the Kruskal coordinates, which allow the maximal extension of the Schwarzschild geometry, we have shown how to embed projections of the Schwarzschild wormhole as a surfaces of revolution in  $\mathbb{R}^3$  for various spacelike slices  $v(u)$ . A foliation of spacetime by a collection of surfaces  $\{v(u)\}$  constitutes a definition of simultaneity. A party of explorers of negligible mass, acting as a collection of test particles, is free to make any such choice, subject only to the constraint,  $|dv/du| < 1$ . For slices of constant Kruskal time, the embeddings trace the time evolution of the wormhole within the Kruskal coordinate system, from its formation at  $v = -1$  to the pinching off at  $v = 1$ , and beyond in the sense of Sec. 5.

However, other choices of  $v(u)$  can push one region of space faster ahead in coordinate time (i.e., Kruskal time) than others, at the option of the party of explorers. In Sec. 6, we showed how one choice of evolving hypersurfaces of simultaneity leads to a separation into three universes, in the limit as the hypersurfaces approach the singularity tangentially. More generally, multiple universes could arise through evolving hypersurfaces approaching  $r = 0$  at multiple tangent points. Spacetime is four dimensional and the slices are only three dimensional. There are no physically correct or incorrect choices. Each one reveals only part of the intricate geometry of the wormhole.

## References

- [1] A. Einstein and N. Rosen, “The particle problem in the general theory of relativity”, Phys. Rev. **48**, 73-77 (1935).
- [2] M. S. Morris and K. S. Thorne, “Wormholes in spacetime and their use for interstellar travel: A tool for teaching general relativity,” Am J. Phys . **56**, 395-412 (1988).
- [3] M. Visser, *Lorentzian Wormholes: From Einstein To Hawking*, (American Institute of Physics Press, New York, 1996)
- [4] J. R. Oppenheimer and H. Snyder, “On continued gravitational contraction” Phys. Rev. **56**, 455-459 (1939).
- [5] R. W. Fuller and J. A. Wheeler, “Causality and multiply connected spacetime”, Phys. Rev. **128**, 919-929 (1962).
- [6] M. Kruskal, “Maximal extension of Schwarzschild metric”, Phys. Rev. **119**, 1743-1745 (1960).
- [7] G. Szekeres “On the singularities of a Riemannian manifold” , Publ. Math. Debrecen **7**, 285-301 (1960). Reproduced in Gen. Relativ. Gravit. **34**, 2001-2016 (2002).
- [8] C. W. Misner, K. S. Thorne, and J. A. Wheeler, *Gravitation* (W. H. Freeman, San Francisco, 1973)
- [9] See the caption of Fig. 31.6, p. 839 of ref. [8]
- [10] B. K. Harrison, K. S. Thorne, M. Wakano, and J. A. Wheeler, *Gravitation Theory and Gravitational Collapse*, (University of Chicago Press, Chicago, 1965)
- [11] A. P. Lightman, W. H. Press, R. H. Price, and S. A. Teukolsky, *Problem book in relativity and gravitation* (Princeton U. Press, Princeton, 1975), p. 90 and p.425.
- [12] Several general relativity textbooks include plots of the Schwarzschild wormhole but calculate only the elementary embedding at Kruskal time  $v = 0$ . For example [3], [8], and L. Ryder, *Introduction to General Relativity* (Cambridge U. Press, Cambridge, 2009); M. P. Hobson, G. P. Efstathiou, and A. N. Lasenby, *General Relativity, an Introduction for Physicists* (Cambridge U. Press, Cambridge, 2006); S. Carroll, *Spacetime and Geometry, an Introduction to General Relativity* (Addison-Wesley, San Francisco, 2004); R. M. Wald, *General Relativity* (University of Chicago Press, 1984).
- [13] R. M. Corless, G. H. Gonnet, D. E. G. Hare, D. J. Jeffrey, and D. E. Knuth, “On the Lambert W function,” Adv. Computational Math. **5**, 329-359 (1996).



- [14] M. P. Hobson, G. P. Efstathiou, and A. N. Lasenby, *General Relativity, an Introduction for Physicists* (Cambridge U. Press, Cambridge, 2006)
- [15] B. O'Neill, *Elementary Differential Geometry* Rev.2nd ed. (Elsevier Academic Press, San Diego, 2006)
- [16] This restriction was not observed in S. Carroll's excellent textbook, *Spacetime and Geometry, an Introduction to General Relativity* (Addison-Wesley, San Francisco, 2004). Slices A and B in Fig. 5.14, p. 228, are inappropriate in that they do not meet the singularity hyperbola tangentially (and the parts 'inside'  $r = 0$  have no meaning). Thus they do not result in the corresponding embeddings in Fig. 5.15. Similar errors occur in Fuller and Wheeler, Ref. [5] Fig. 3 (1) and (5). However, these errors were corrected in Fig. 31.6, p. 839 of Ref. [8].
- [17] More generally one can show, using Eq. (4.22) of Ref. [13], that if a spacelike slice  $v(u)$ , has the Taylor expansion about a point  $u_1$  given by,  $v(u) = v_s(u_1) + [u_1/v_s(u_1)](u - u_1) + [v''(u_1)/2](u - u_1)^2 + O((u - u_1)^3)$ , and thus meets the singularity hyperbola,  $v_s(u)$ , tangentially at  $u_1$ , then  $dg/du \sim C/\sqrt{|u - u_1|}$ , in an open interval containing  $u_1$ , where  $C$  is a positive constant, provided  $v''(u_1) < 1/(1 + u_1^2)^{3/2}$ .